

# Physical aspects of skin dose distribution in tomotherapy of breast cancer

P. Saadatmand<sup>1</sup>, S.R. Mahdavi<sup>1,2\*</sup>, A. Nikoofar<sup>3</sup>, G. Esmaili<sup>4</sup>, M. Jalilifar<sup>1</sup>, S. Khazaie<sup>1</sup>, S. Vejdani<sup>5</sup>

<sup>1</sup>Department of Medical Physics, School of Medicine, Iran University of Medical Sciences, Tehran, Iran

<sup>2</sup>Radiation Biology Research Center, Iran University of Medical Sciences, Tehran, Iran

<sup>3</sup>Department of Radiation Oncology, School of Medicine, Iran University of Medical Sciences, Tehran, Iran

<sup>4</sup>Radiotherapy Department, Pars Hospital, Tehran, Iran

<sup>5</sup>Department of Radiation Oncology, Firoozgar Hospital, Iran University of Medical Sciences, Tehran, Iran

## ABSTRACT

### ► Original article

**\*Corresponding author:**

Seied Rabi Mahdavi, Ph.D.,

**E-mail:**

[srmahdavi@hotmail.com](mailto:srmahdavi@hotmail.com)

**Received:** October 2023

**Final revised:** March 2024

**Accepted:** April 2024

*Int. J. Radiat. Res.*, January 2025;  
23(1): 83-90

DOI: 10.61186/ijrr.23.1.83

**Keywords:** Tomotherapy, intensity-modulated radiotherapy, skin dose, breast cancer.

**Background:** Estimating the accuracy of Treatment Planning Systems (TPS) in skin dose calculation is essential to achieving the intended therapeutic outcomes in breast cancer radiotherapy. This study aims to validate tomotherapy TPS accuracy in skin dose estimation. **Materials and Methods:** The ability of Accuray Precision TPS to provide precise skin dose calculations was examined by utilizing the Gafchromic EBT3 film, which was placed on the surface of the cylinder Delta4 phantom. The target volume received a 2Gy dose following setup validation. The accuracy of TPS was assessed using distinct spatial resolutions for dose calculation in helical and direct Tomotherapy plans. Using the RIT software, gamma analysis was employed to evaluate the precision of TPS skin dose distribution relative to the EBT3 film. **Results:** Comparison of skin dose distribution between the TPS and EBT3 films demonstrated acceptable gamma passing rates for helical (up to 98.51%) and direct plan (up to 90.41%) using gamma index criteria of 5 mm/5%. However, the gamma index of helical and direct tomotherapy plans with passing criteria of 3 mm/3% was 84.15% and 79.12%, respectively. Our findings indicate satisfactory consistency (3-5%) between measured and calculated skin doses using the EBT3 film and TPS, employing "high" spatial resolution dose calculation in helical and direct Tomotherapy plans. **Conclusion:** The reliability of the tomotherapy TPS in skin dose calculation is maintained by utilizing high spatial resolution for dose computation. The accuracy of TPS validated against the Gafchromic EBT3 film was within an acceptable gamma-passing rate.

## INTRODUCTION

Tomotherapy, a modern form of Radiation Therapy (RT) technique, is employed as an adjuvant treatment for breast cancer using the Tomo Direct or Helical mode <sup>(1)</sup>. This method utilizes modulated X-ray fan beams to achieve superior dose conformity and organ sparing compared to conventional methods <sup>(2)</sup>.

To optimize the efficacy of radiotherapy, it is imperative to irradiate sufficiently the surgical scar and superficial regions when the tumor extends near the skin, aiming to eliminate malignant cells and minimize the risk of recurrence <sup>(3-5)</sup>. However, excessive skin radiation can induce radiation-induced skin toxicity due to the skin's rapid cellular turnover rate and high radiosensitivity <sup>(6, 7)</sup>, impacting the patient's quality of life and potentially causing treatment interruption <sup>(8)</sup>. Given this, precise calculation of the skin dose distribution within Treatment Planning Systems (TPS) plays a vital role

in ensuring adequate target volume coverage and mitigating skin toxicity <sup>(9)</sup>.

Several investigations have assessed TPS accuracy in calculating the surface dose during Tomotherapy, employing TLD <sup>(10-16)</sup>, Gafchromic EBT film <sup>(17-19)</sup>, MOSFET <sup>(16, 17, 20)</sup>, and MOSFET-based skin solid-state dosimeter (MOSkin) <sup>(18)</sup> detectors. However, the results were inconsistent, indicating agreement and disagreement between the TPS-calculated and measured doses in different studies <sup>(21)</sup>. Furthermore, skin dosimetry complexity in breast radiotherapy requires high-resolution dosimeters due to curved structures, inhomogeneous dose distribution, steep dose gradient, and lack of electron equilibrium at the surface <sup>(22)</sup>. The Gafchromic EBT film stands out among the available dosimeters as a suitable choice, providing accurate two-dimensional (2D) surface dose mapping with high resolution <sup>(23)</sup>.

Based on the information available, previous investigations have assessed TPS accuracy at the surface using the dose difference parameter.

However considering a 10% uncertainty in the measured dose of high-gradient regions, spatial displacement should be evaluated alongside dose differences<sup>(21)</sup>. The present study uniquely focuses on assessing the accuracy of the calculated skin dose distribution of the tomotherapy TPS compared to the Gafchromic EBT3 film's measured dose distribution utilizing gamma analysis. Gamma analysis assesses global and local similarity between planned and measured dose distributions, dose magnitude, and spatial distribution by combining dose differences and distance to agreement parameters. This approach, utilizing high-resolution dosimetry and a sophisticated analysis method, addresses a significant gap in the current literature and offers valuable insights into the reliability of the tomotherapy TPS in accurately predicting skin dose distribution during breast cancer radiotherapy.

## MATERIALS AND METHODS

The accuracy of the tomotherapy TPS dose calculation algorithm on the surface and depth regions was evaluated using the EBT3 Gafchromic film and diode detectors inside the Delta4 phantom, respectively, during breast cancer tomotherapy.

### Treatment Planning of Delta4 Phantom

A cylinder Delta4 phantom (ScandiDos AB, Uppsala, Sweden) was employed for breast cancer tomotherapy simulation. This phantom, with a diameter of 22 cm and a length of 40 cm, is employed for quality assurance (QA) evaluation. It consists of polymethyl methacrylate (PMMA) with a relative electron density of 1.147 g/cc and contains 1069 diodes located in two sagittal and coronal planes perpendicularly. The computed tomography (CT) images of the Delta4 phantom and the accompanying HU/density table provided by ScandiDos were sent to the tomotherapy TPS (Accuray Inc., Sunnyvale, CA) for the treatment planning procedure. Using a threshold density of 0.55 g/cm<sup>3</sup>, the TPS automatically detected and generated the skin contour. The superficial planning target volume (PTV) was segmented, with its anterior boundary 5 mm below the surface of the phantom.

An automatic delineation process generates a 2 mm thick surface layer (SL2) along the whole PTV, as indicated in figure 1. Tomotherapy planning software was utilized to create helical and direct tomotherapy plans, with a prescription of 50 Gy in 25 fractions. The Tomo direct plan was created by incorporating a set of five gantry angles: 31.7, 125, 315, 318, and 128. A pitch of 0.287, a modulation factor of 2.8, and a field width of 2.5 were chosen for treatment. Different spatial resolutions accessible in the TPS were utilized for dose calculations. Before treatment, a QA process was performed to ensure precise delivery of the

planned dose. The QA plans were created by overlaying the patient (here, the Delta4 phantom) treatment plans on the Delta4 phantom CT image series in the TPS, implying that the Delta4 phantom CT images were regarded as both the patient and the phantom. As a result, the QA plan encompassed rescaling the original plan into a single fraction plan while keeping the dose distribution intact.

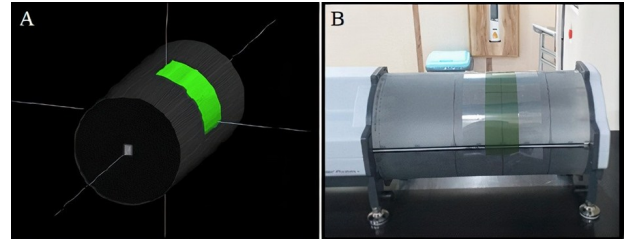


**Figure 1.** (A) The Delta 4 phantom three-dimensional reconstruction in the treatment planning system after contouring a 2 mm thick superficial layer (green color) adjacent to the PTV and (B) placing the experimental EBT3 film on the Delta 4 phantom's surface corresponding to the SL2 segment for skin dosimetry.

### Calibration of the EBT3 Gafchromic film

In this study, the skin dose was assessed using the EBT3 film (Ashland ISP, Wayne, USA), a new Gafchromic film with a 153 $\mu$ m effective point of measurement, characterized by features like tissue similarity, high spatial resolution, and low energy sensitivity<sup>(24)</sup>. Film handling followed the guidelines provided in the American Association of Physicists in Medicine (AAPM) TG-235 report.

Film calibration utilized a 30 cm diameter, 18 cm thick cylindrical Cheese phantom (Gammex RMI, Middleton, WI) with a density of 1.047 g/cc. CT scans (Siemens 64-Slice) of the cylindrical phantom were conducted at Pars Hospital in Tehran, Iran, using a 2 mm slice thickness, followed by electronic transfer of CT images to the TPS. Regarding the independence of the film response from the calibration method, as Avanzo et al.<sup>(15)</sup> indicated, EBT3 film calibration was conducted using direct plans. In total, 39 calibration films, each with dimensions of 1.5 $\times$ 1.5 cm<sup>2</sup>, were prepared and grouped into 13 groups. Every group of films underwent irradiation using individual Tomo Direct plans on the Tomotherapy system (Radixact, Accuray Inc., Sunnyvale, CA), with distinct prescribed doses to generate a calibration curve encompassing the 20-570 cGy spectrum. The absolute dose of each plan was measured with a Tomo electrometer and a 0.053 cm<sup>3</sup> Exradin A1SL ionization chamber (Standard Imaging) located in the cylindrical phantom hole. A calibration curve was generated by relating the mean analog-to-digital (A/D) value of scanned images of irradiated calibration films with the Exradin A1SL ionization chamber's measured dose at different dose levels.

### Phantom dose delivery

The pretreatment Mega-Voltage Computed

Tomography (MVCT) images were taken from the Delta4 phantom for setup verification, encompassing the entire PTV with a 2 mm slice thickness. Then, the MVCT images were registered with the planning CT images using a bone registration algorithm. Registration was assessed visually through a checkerboard arrangement, which includes a partially transparent image overlay to showcase both images, functioning as a manual approach to evaluate the automatic registration's quality. The essential shifts obtained from the registration results were applied to place the Delta4 phantom in the correct position. These processes were repeated before each treatment delivery for setup confirmation.

### **Pretreatment QA with Delta4 phantom**

The pre-treatment QA process is imperative to validate the accuracy of the delivered dose distribution before initiating treatment. The QA treatment plan and radiation dose were exported from the TPS in DICOM RT format and later imported into the Delta4 software (25). The assessment of conformity between the planned and delivered dose distributions was conducted using the Delta4 software, employing the gamma-passing rate (GPR). The GPR quantifies the percentage of points in a dose distribution that satisfies predefined criteria for dose difference (DD), which is the absolute dose discrepancy between planned and measured doses, and distance to agreement (DTA) parameters, which is the minimum distance between the corresponding dose points. The three-dimensional (3D) GPR of helical and direct plans was assessed through the Delta4 software, with the benchmark being 3% DD, 3 mm DTA, and 90% GPR. The attainment of the gamma index, which integrates DD and DTA to evaluate the agreement between calculated and measured dose distributions, was realized through equation 1.

$$\gamma = \sqrt{\frac{(\Delta r)^2}{(DTA)^2} + \frac{(\Delta D)^2}{(DD)^2}} \quad (1)$$

Where;  $\Delta r$  is the distance between the corresponding points in the calculated and measured dose distributions and the parameter  $\Delta D$  is the absolute dose difference between the calculated and measured dose distributions at each point. Passed points are indicated by  $\gamma \leq 1$  (26).

### **Film analysis**

Utilizing the Vidar scanner, film scanning was conducted at a pixel measurement of 0.178 mm while benefiting from an automatic self-calibration function that ensured stability and sufficient warming of the light source. However, the Vidar scanner's performance was evaluated before being used based on the calibration guidelines recommended by the manufacturers.

The calibration and experimental films were positioned for scanning in the Vidar scanner utilizing

a 21×29.7 cm<sup>2</sup> binding cover template due to the scanner's restrictions on films with dimensions less than 15.24 cm in length and 17.78 cm in width, as depicted in figure 2. Calibration and experimental film templates consisted of 39 holes (13 rows and 3 columns) of 1.5×1.5 cm<sup>2</sup> and 3 holes (3 rows) of 6×16 cm<sup>2</sup>, respectively. The films were taped onto the holes to allow for reading, as demonstrated in figure 2. The calibration films' background optical density was measured by scanning unexposed films 24 hours before exposure. Following the guidelines of AAPM TG-235, all films were stored in an appropriate environment for up to 36 hours after exposure and before the analysis. The scanned films were saved as 16-bit grayscale images (\*.rv4 format) and assessed with the RIT113 V5.0 software (Radiological Imaging Technology, Colorado Springs, CO). Following the RIT's recommendation, a 5×5 median filter removed image noise and artifacts. A region of interest (ROI) of 5×5 mm<sup>2</sup> was placed centrally on calibration films, and the RIT software displayed average A/D values. Correlating the mean A/D values of the exposed films with the Exradin A1SL ionization chamber's measured dose yielded a dose calibration curve using a piecewise polynomial correlation in the RIT software. The RIT software applied the dose calibration curve to the experimental film to evaluate the skin dose.

### **Skin dose measurement**

The experimental films (6×16 cm<sup>2</sup>) were placed on the phantom's surface for skin dosimetry, corresponding to the SL2 segment in figure 1. Each treatment plan was delivered three times following the setup verification, and skin dosimetry was repeated three times. Each experimental film was scanned five times using the Vidar (Herndon, VA) Dosimetry PRO Advantage (Red) scanner.

### **TPS skin dose map**

The Helical and direct tomotherapy plan's 3D dose distributions were exported in the DICOM RT format from the TPS. Utilizing the Matlab software (MathWorks, Natick, MA), a skin dose map (SDM<sub>plot</sub>) was extracted from the 3D dose distribution for comparison with the 2D dose distribution of the EBT3 film (SDM<sub>film</sub>).

### **Statistical analysis**

The TPS algorithm's precision was assessed by comparing the mean skin dose calculated by the TPS with that obtained from the EBT3 film. The computation of the percentage difference (%Diff) between the calculated and measured doses was achieved through equation 2 (27).

$$\%Diff = \frac{(D_{cal} - D_{meas})}{D_{meas}} \times 100 \quad (2)$$

Where  $D_{cal}$  denotes the calculated dose by TPS, and  $D_{meas}$  represents the measured dose by the EBT3

film.

The measurement uncertainty was derived from the standard deviation of five readings and the three films exposed for each plan using SPSS Version 27 (IBM Corp., Armonk, NY) (28). Using 2D GPR analysis in the RIT software, a comparison was made between the  $SDM_{plan}$  and the  $SDM_{film}$ , with 3 mm/3%, 5 mm/5% criteria, and 90% GPR. Through the implementation of rigid body registration, both images were matched for gamma analysis by identifying five "control points" on the " $SDM_{plan}$ " and " $SDM_{film}$ " within the RIT software. The gamma analysis was carried out between two dose maps with the assistance of the "Patient QA Analysis" option within the RIT software.

### RESULTS

Figures 2A and B, visually presents the template of calibration films subjected to prescribed doses ranging from 20 to 570 cGy before and during scanning with the Vidar scanner. Figures 2C and D show scanned images of the calibration films labeled with the measured dose of the Exradin A1SL ionization chamber and the calibration curve of the Gafchromic EBT3 film created by the RIT software, respectively. Verification of the Vidar scanner's performance, following manufacturer-recommended calibration protocols.

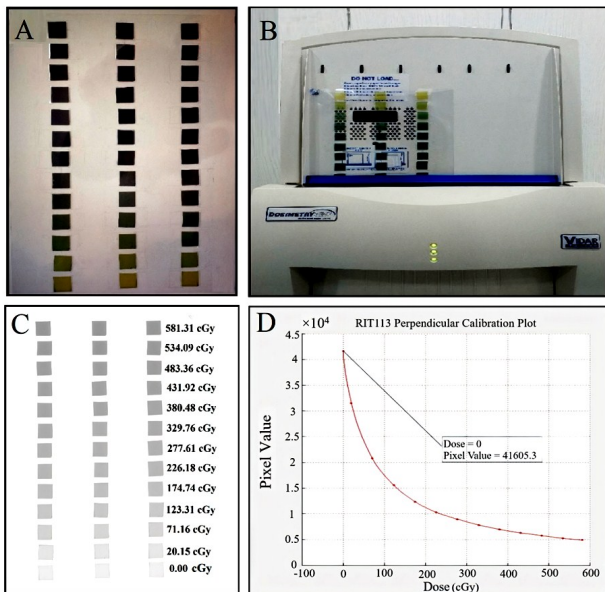


**Figure 2.** (A) The template of calibration films consists of 39 films of 1.5x1.5 cm<sup>2</sup> in 13 groups of 3 irradiated with specified prescribed doses in the dose range 0-570 cGy. (B) Scanning a template film with a Vidar scanner. (C) The scanned image of the calibration films labeled with the doses measured with the Exradin A1SL ionization chamber. (D) The Gafchromic EBT3 film calibration curve from the RIT software.

Figure 3 displays the Delta4 phantom dose distributions of helical and direct tomotherapy plans, ensuring a 95% isodose curve (red color) covers the target volume positioned 5mm below.

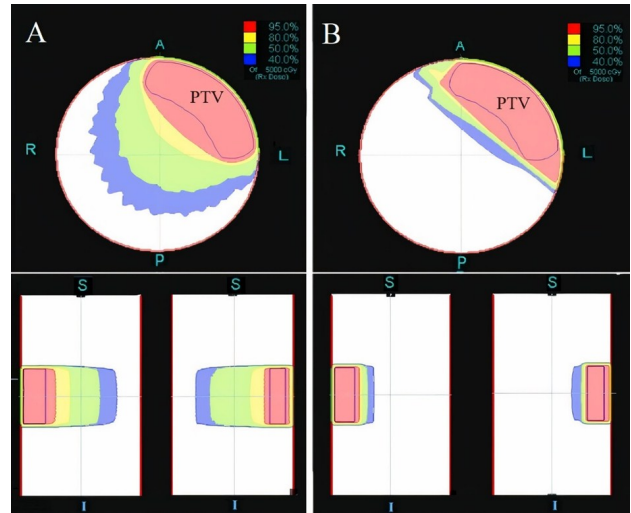


**Figure 3.** The isodose distribution in axial, sagittal, and coronal views for (A) helical and (B) direct Tomotherapy plans, with a superficial target volume 5 mm below the phantom surface for simulation of breast cancer treatment.

### Dosimetric verification of TPS plan

Using gamma analysis in the Delta4 software, a pre-treatment QA procedure was performed to ensure the precise delivery of the planned dose. Figure 4 illustrates gamma index maps representing blue transitions ( $\gamma < 1$ ) and red failures ( $\gamma > 1$ ), along with isodose line comparisons in the horizontal and vertical detector planes of the Delta4 phantom for helical and direct tomotherapy plans.

The accuracy of dose delivery following the AAPM TG-119 recommendation was confirmed by the 99.6% and 99.3% 3D GPRs with passing criteria of 3mm/3% for helical and direct tomotherapy plans, respectively, as shown in figure 4.

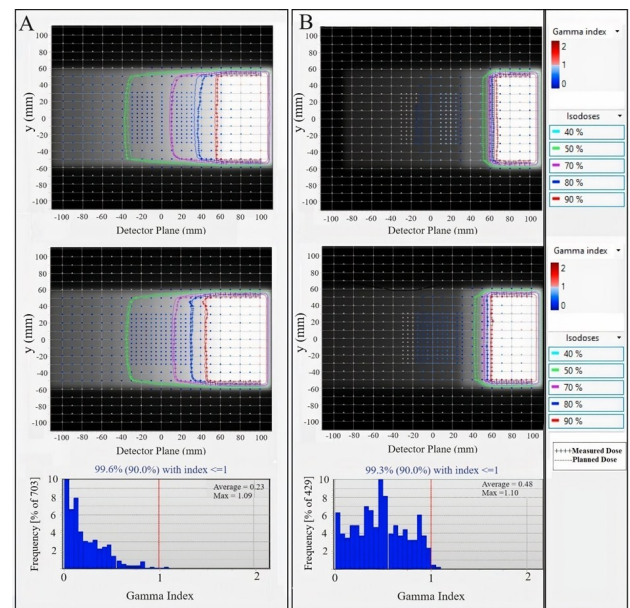


**Figure 4.** The isodose line comparisons and gamma index maps between calculated and measured doses in the horizontal and vertical detector planes of the Delta4 phantom and gamma graphs are shown from top to bottom in (A) helical and (B) direct tomotherapy plans. The Gamma index maps denote blue transitions (gamma < 1) and red failures (gamma > 1). The gamma-passing rate (3%/3 mm) for both plans was over 90%.

### Skin dose measurement results

The skin dose comparison between the EBT3 film and the TPS is demonstrated in table 1. The helical plan exhibits a higher measured skin dose (up to 6.61%) than the direct plan. The skin dose disparity between the plan and the EBT3 film, using high spatial resolution dose calculation in both helical and direct plans, remained within the 3-5% range. However, the tomotherapy TPS overestimates skin dose in helical (up to 21.08%) and direct (up to 27.16%) planes with a coarser dose grid.

The  $SDM_{plan}$  was extracted via the Matlab software from the 3D skin dose distribution, which was generated using a high spatial resolution of dose calculation. Gamma analysis was employed to evaluate the TPS skin dose accuracy against the EBT3

film, considering global and local precision, including dose magnitude and spatial distribution. Figure 5 visualizes the  $SDM_{film}$ ,  $SDM_{plan}$ , and the gamma image for helical and direct tomotherapy plans. The gamma image visually represents the level of agreement between these two distributions by color-coding points based on a gamma-passing criterion of 3 mm/3%. In comparing the  $SDM_{film}$  to the  $SDM_{plan}$ , the 2D GPR with a 3mm/3% criterion was 84.15% for helical and 79.12% for direct tomotherapy plans (figure 6). Nonetheless, using the 5 mm/5% criterion resulted in passed 2D GPR for helical (up to 98.51%) and direct (up to 90.41%) tomotherapy plans (figure 6). The Gamma passing percent represents pixels with gamma 0 to 1.

**Table 1.** Skin dose results by the EBT3 film and the TPS dose calculation in helical and direct tomotherapy plans

Plan mode	EBT3 Film dose (cGy)	TPS-high grid dose (cGy)	TPS-medium grid dose (cGy)	TPS-low grid dose (cGy)	TPS-very low grid dose (cGy)	%Diff of EBT3 with TPS			
						High grid	Medium grid	Low grid	Very low
Helical	128.84±0.83	134	142	152	156	4.01%	10.94%	18.02%	21.08%
Direct	120.32±0.67	126	134	147	153	4.72%	11.37%	22.17%	27.16%

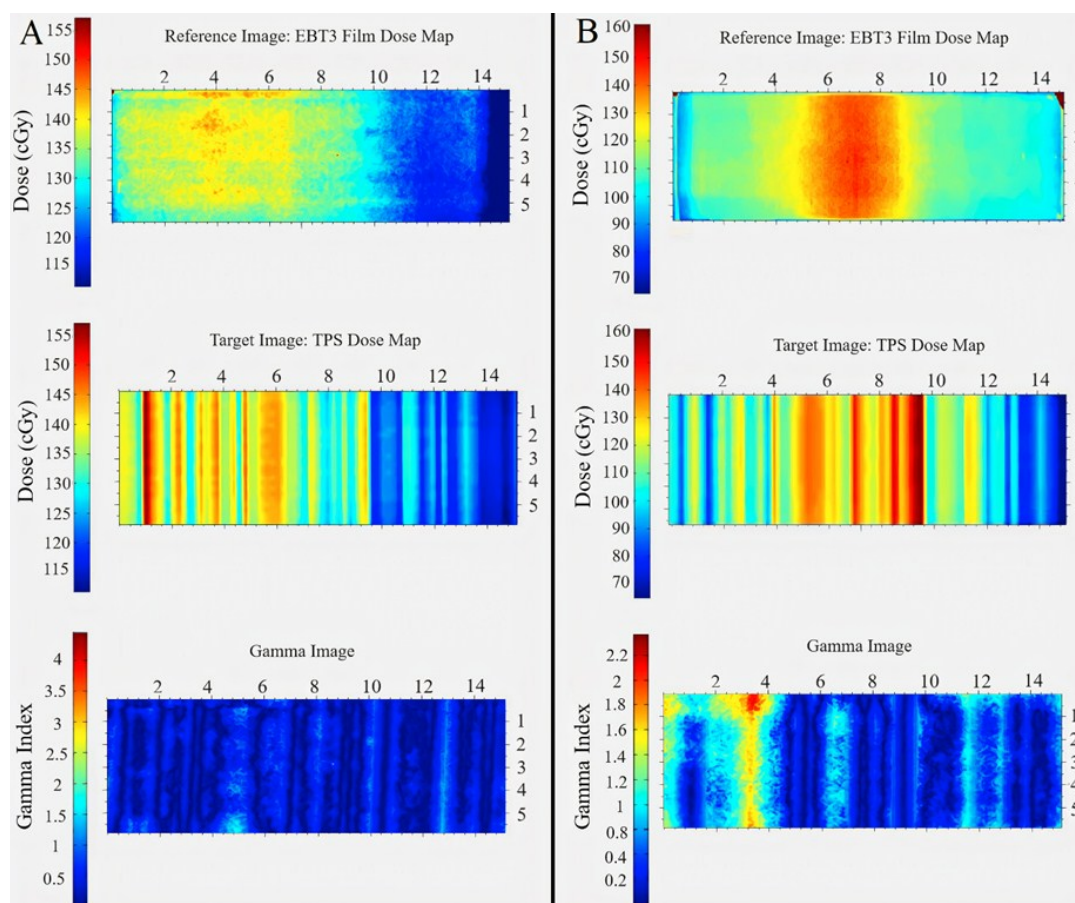


**Figure 5.** Comparison between the EBT3 film's dose map ( $SDM_{film}$ ) and the TPS-calculated dose map ( $SDM_{plan}$ ) along with a two-dimensional gamma image (3%/3 mm) for both helical (A) and direct tomotherapy plans.

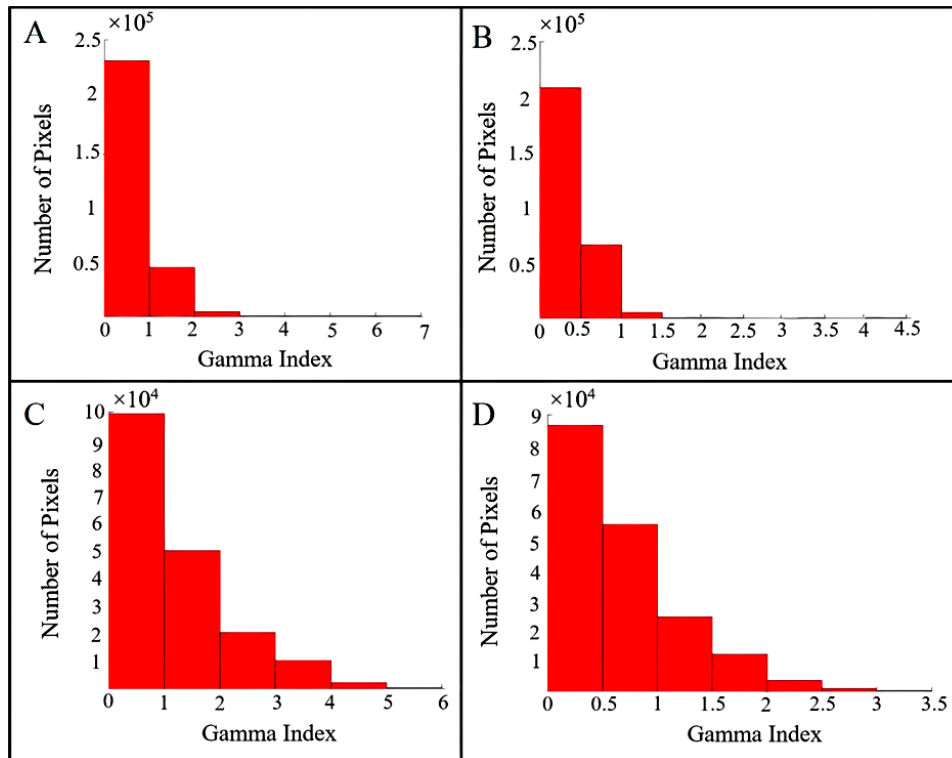


**Figure 6.** Histogram of two-dimensional gamma analysis between the SDM film and the SDM plan for (A) the helical tomotherapy plan with the passing criteria of 3 mm/3% and (B) 5 mm/5% and (C) direct tomotherapy plan with the passing criteria of 3mm/3% and (D) 5mm/5%.

## DISCUSSION

Estimating the precision of TPS in skin dose calculation offers crucial clinical insights into breast cancer patients and allows treatment planning optimization to avoid skin toxicity and tumor recurrence (21). This investigation aimed to validate the TPS's ability to accurately predict skin dose by employing the Gafchromic EBT3 film on the Delta4 phantom's surface under geometric and scattering conditions similar to those in the breast cancer tomotherapy. Phantom controls patient-specific factors like respiratory movement uncertainties. Additionally, it manages the effect of the temperature difference between the calibration settings and the patient's skin due to the temperature dependence of the film, influencing film dosimetry accuracy (15). The Delta4 phantom allows assessing the 3D dose distribution in deep regions over alternative phantoms. However, its software's limitations prevent surface dose assessment due to a smaller delivered dose volume than the phantom's. Thus, the TPS skin dose accuracy was verified using the EBT3 Gafchromic film at an effective measuring point around 70  $\mu\text{m}$  depth, aligning with the International Commission on Radiation Units and Measurements (ICRU) skin dosimetry suggestion (29, 30). The Gafchromic EBT3 provides a precise skin dose assessment due to its high spatial resolution and ability to capture complex dose gradients, making it invaluable for monitoring radiation exposure to the surface (21). The application of the parallel plate

ionization chamber for surface dosimetry was restricted by its small resolution, time-consuming measurement, and unavailability in all institutions (22). Furthermore, while TLDs offer good dose resolution, they are limited to measuring point-to-point doses (22) and their small size presents challenges in the accurate TPS tracking (14). Also, TLD, OSLD, and MOSFET were used at 1-2 mm depth, differing from ICRU's 70  $\mu\text{m}$  clinical skin dosimetry depth (29, 30).

Consistent with an earlier investigation, the present study demonstrated a 3-5% agreement in the mean skin dose between the EBT3 film and the TPS, employing high spatial resolution of dose calculation (18, 21, 31). In the high spatial resolution mode of TPS, the resolution of the dose calculation aligns with that of the imported CT data, whereas medium, low, and very low dose grid sizes result in dose calculations for every 2 $\times$ 2, 4 $\times$ 4, and 8 $\times$ 8 imported CT voxels in the axial image, respectively. Moreover, prior Monte Carlo simulations showed the tomotherapy TPS algorithm's ability to precisely calculate initial body millimeters, even in the presence of inhomogeneities (32, 33). Still, certain earlier investigations revealed an overestimation exceeding 5% in the average surface dose of the TPS compared with the TLD (10-16, 34), the MOSFET (16, 17), the MOSkin (35), and the Gafchromic EBT film (15, 17, 19) assessments in both phantoms and in vivo studies. This overestimation is in agreement with the results of this study when employing a coarser dose calculation grid. Therefore, the TPS accuracy in the surface dose calculation is enhanced

by adopting a grid resolution corresponding to the imported CT data, as stated by Avanzo *et al.* (15). For controlling the surface dose overestimation with a coarser calculation grid, a boost is required to raise the surface dose if the target extends to the surface (18). Wang *et al.* reported an underestimating skin dose calculation (up to 14%) using the Monte Carlo simulations in Varian Eclipse TPS. Nevertheless, they increased the skin dose accuracy to an acceptable level by extending the body surface contour by 1 to 2 cm and moving the entry point away from the skin, where the model-based calculation algorithm encounters inaccuracies (36). Furthermore, considering a 10% uncertainty in the measured dose of high-gradient regions using only the DD criteria (21), a cautious interpretation of results in such a critical region is recommended. Thus, for the precise comparison of the TPS data and the measured dose in high-gradient regions, spatial displacement should be evaluated alongside dose differences (21). Zani *et al.* assessed the precision of superficial dose calculations by the tomotherapy TPS in various Head & Neck plans using the Gafchromic EBT3 films on the Alderson RANDO phantom. They considered both distance to the agreement and dose difference results, indicating measured doses lower than the TPS calculation (up to 16%), with a maximum DTA value of 1.5 mm, indicating the HT TPS's precise superficial dose estimation (21). In a heterogeneous phantom, Sterpin *et al.* recorded a 3%/2 mm discrepancy in the superficial dose in assessing the tomotherapy TPS convolution/superposition algorithm with the EBT film dose profiles (32). We performed a gamma analysis that combines the DD and the DTA to assess the similarity between planned and measured dose distributions. It produces a GPR as the percentage of points in a dose distribution that satisfies predefined criteria for the DD and the DTA. The accuracy of planned dose delivery on the Delta4 phantom was verified via the 3D GPR of more than 95% in-depth regions, using the 3%/3mm criterion, in both helical and direct tomotherapy plans. Slight discrepancies likely arise from the diodes' small grid resolution, resulting in inaccuracies in the energy flux estimation for dose calculation (37). A 2D GPR below 90% with 3%/3 mm was observed between the EBT3 film measured and the calculated skin dose map, whereas the 5%/5 mm criterion yielded a gamma index over 90% for both helical and direct delivery modes. Factors such as image misregistration in the RIT software, setup inaccuracies, TPS skin mispositioning, and varying voxel densities due to the limited CT resolution may cause a decline in the GPR between the calculated and measured skin dose maps (38). Toosi *et al.* stated that differences in film positioning inside the phantom and on its surface during calibration and skin dosimetry are involved in the discrepancy between measured and calculated doses (24). Additional factors, such as the TPS dose

calculation algorithm's inability to incorporate electron contamination effects, inaccuracies in the convolution-superposition algorithm's dose kernel near the surface, and the discretization of every helical plane rotation into 51 equally spaced angles, can affect the TPS dose accuracy, leading to disparities with film doses (15, 29). The ICRU report 83 recommends the 5%/5mm gamma index (39, 40), for the skin dose assessment, which is above the clinical norm, but skin's steep dose gradients, skin contour changes, and inherent uncertainties (detector, setup, modeling) on the TPS dose calculation variation make less stringent criteria still acceptable.

This study shows that more tangential fields in the helical delivery mode cause a higher skin dose (up to 6.61%) than in the direct delivery mode. The deviation between the planned and measured doses is higher (up to 28.84%) in the direct mode, possibly due to a greater dose gradient caused by more normal incident beams (15). There has been no substantial variation in measurement-calculation agreement with modulation factor quantities (21). In future studies, it is important to acknowledge certain limitations. Our study was conducted within a controlled environment, potentially overlooking real-world complexities. Inter-fractional changes and patient setup variability were not fully accounted for. Subsequent research must address our study's constraints, such as the controlled phantom environment and the potential role of anatomical changes, patient setup variations, and beam modeling parameters in determining the accuracy of the TPS for skin dose estimation.

## CONCLUSION

The EBT3 Gafchromic film is a suitable detector for surface dose measurements in the tomotherapy treatment. The Accuray Precision dose calculation engine in the high spatial resolution mode showed acceptable accuracy for the skin dose assessment against the Gafchromic EBT3 film. However, using a coarser dose calculation grid, the TPS overestimates the skin dose in the tomotherapy treatment. Assessing the accuracy of the TPS in the skin dose calculation in the breast cancer tomotherapy can provide *valuable* information for clinical consideration.

## ACKNOWLEDGMENTS

*The Iran University of Medical Sciences supported this report (research project: 1400-1-104-21280). The authors have special thanks to the Pars Hospital radiotherapy department crew for their cooperation and very useful experiments.*

**Funding:** The Iran University of Medical Sciences under grant number 21280 supported this study.

**Conflicts of interest:** The authors have no conflicts of

interest.

**Ethical consideration:** This study was reviewed and approved under institutional Ethics Committee approval (IR.IUMS.FMD.REC.1400.591).

**Author contributions:** PS, SRM, and AN designed the project. SRM and GE planned the treatments, and PS, MJ, and SKH contributed to the acquisition of the data. AN and SV contributed to the clinical criteria. PS and SKH processed the data and conducted statistical analyses. PS wrote the manuscript with input from SRM, AN, GE, MJ, SKH, and SV. SRM was the senior author, supervising the project. All authors contributed to the article and approved the submitted version.

## REFERENCES

- Crop F, Pasquier D, Baczkiewicz A, et al. (2016) Surface imaging, laser positioning or volumetric imaging for breast cancer with nodal involvement treated by helical TomoTherapy. *J Appl Clin Med Phys*, **17(5)**: 200-11.
- Lauche O and Kirova YM (2014) Helical tomotherapy in breast cancer treatment. *Breast Cancer Manag*, **3(5)**: 441-9.
- Parsai El, Shvydka D, Pearson D, et al. (2008) Surface and build-up region dose analysis for clinical radiotherapy photon beams. *Appl Radiat Isot*, **66(10)**: 1438-42.
- Akino Y, Das IJ, Bartlett GK, et al. (2013) Evaluation of superficial dosimetry between treatment planning system and measurement for several breast cancer treatment techniques. *Med Phys*, **40(1)**: 011714.
- Panettieri V, Barsoum P, Westermarck M, et al. (2009) AAA and PBC calculation accuracy in the surface build-up region in tangential beam treatments. Phantom and breast case study with the Monte Carlo code PENELOPE. *Radiother Oncol*, **93(1)**: 94-101.
- Chen M-F, Chen W-C, Lai C-H, et al. (2010) Predictive factors of radiation-induced skin toxicity in breast cancer patients. *BMC Cancer*, **10(1)**: 1-9.
- Xie Y, Wang Q, Hu T, et al. (2021) Risk Factors Related to Acute Radiation Dermatitis in Breast Cancer Patients After Radiotherapy: A Systematic Review and Meta-Analysis. *Front Oncol*, **29(11)**: 738851.
- Mori M, Cattaneo G, Dell'Oca I, et al. (2019) Skin DVHs predict cutaneous toxicity in Head and Neck Cancer patients treated with Tomotherapy. *Phys Med*, **59**: 133-41.
- Farhood B, Toossi MTB, Soleymanifard S, et al. (2017) Assessment of the accuracy of dose calculation in the build-up region of the tangential field of the breast for a radiotherapy treatment planning system. *Contemp Oncol (Pozn)*, **21(3)**: 232-9.
- Capelle L, Warkentin H, MacKenzie M, et al. (2012) Skin-sparing Helical Tomotherapy vs 3D-conformal radiotherapy for adjuvant breast radiotherapy: in vivo skin dosimetry study. *Int J Radiat Oncol Biol Phys*, **83(5)**: e583-e90.
- Zibold F, Sterzing F, Sroka-Perez G, et al. (2009) Surface dose in the treatment of breast cancer with helical tomotherapy. *Strahlenther Onkol*, **185(9)**: 574-81.
- Ramsey CR, Seibert RM, Robison B, et al. (2007) Helical tomotherapy superficial dose measurements. *Med Phys*, **34(8)**: 3286-93.
- Kim S-Y, You S-H, Song T-S, et al. (2009) Superficial Dosimetry for Helical Tomotherapy. *Radiat Oncol J*, **27(2)**: 103-10.
- Kowalik A, Konstany E, Piotrowski T, et al. (2019) Calculation and measurement of doses in the surface layers of a phantom when using tomotherapy. *Rep Pract Oncol Radiother*, **24(2)**: 251-62.
- Avanzo M, Drigo A, Kaiser SR, et al. (2013) Dose to the skin in helical tomotherapy: results of in vivo measurements with radiochromic films. *Phys Med*, **29(3)**: 304-11.
- Kinhikar RA, Murthy V, Goel V, et al. (2009) Skin dose measurements using MOSFET and TLD for head and neck patients treated with tomotherapy. *Appl Radiat Isot*, **67(9)**: 1683-5.
- Snir JA, Mosalaei H, Jordan K, et al. (2011) Surface dose measurement for helical tomotherapy. *Med Phys*, **38(6Part1)**: 3104-7.
- Hardcastle N, Soisson E, Metcalfe P, et al. (2008) Dosimetric verification of helical tomotherapy for total scalp irradiation. *Med Phys*, **35(11)**: 5061-8.
- Goddu SM, Yaddanapudi S, Pechenaya OL, et al. (2009) Dosimetric consequences of uncorrected setup errors in helical Tomotherapy treatments of breast-cancer patients. *Radiother Oncol*, **93(1)**: 64-70.
- Cherpak A, Studinski RC, Cygler JE (2008) MOSFET detectors in quality assurance of tomotherapy treatments. *Radiother Oncol*, **86(2)**: 242-50.
- Zani M, Talamonti C, Bucciolini M, et al. (2016) In phantom assessment of superficial doses under TomoTherapy irradiation. *Phys Med*, **32(10)**: 1263-70.
- Aydarous A (2014) Measurement and comparison of skin dose distribution in water phantom exposed to 6 MV photon beam. *J Appl Sci*, **14(17)**: 1952-8.
- Reynolds TA and Higgins P (2015) Surface dose measurements with commonly used detectors: a consistent thickness correction method. *J Appl Clin Med Phys*, **16(5)**: 358-66.
- Toossi MTB, Mohamadian N, Mohammadi M, et al. (2020) Assessment of skin dose in breast cancer radiotherapy: on-phantom measurement and Monte Carlo simulation. *Rep Pract Oncol Radiother*, **25(3)**: 456-61.
- Srivastava RP and De Wagter C (2019) Clinical experience using Delta 4 phantom for pretreatment patient-specific quality assurance in modern radiotherapy. *J Radiother Pract*, **18(2)**: 210-4.
- Li H, Dong L, Zhang L, et al. (2011) Toward a better understanding of the gamma index: Investigation of parameters with a surface-based distance method a. *Med Phys*, **38(12)**: 6730-41.
- Saadatmand P, Amouheidari A, Shanei A, et al. (2020) Dose perturbation due to dental amalgam in the head and neck radiotherapy: a phantom study. *Med Dosim*, **45(2)**: 128-33.
- Saadatmand P, Shanei A, Amouheidari A, et al. (2019) Evaluation of the effects of dental filling material artifacts on IMRT treatment planning in patient with nasopharyngeal cancer. *Int J Radiat Res*, **17(3)**: 477-83.
- McDermott PN (2020) Surface dose and acute skin reactions in external beam breast radiotherapy. *Med Dosim*, **45(2)**: 153-8.
- Clarke R, Fry F, Stather J, et al. (1993) 1990 recommendations of the International Commission on Radiological Protection. *Documents of the NRPB*, **4(1)**: 1-5.
- Tournel K, Verellen D, Duchateau M, et al. (2007) An assessment of the use of skin flashes in helical tomotherapy using phantom and in-vivo dosimetry. *Radiother Oncol*, **84(1)**: 34-9.
- Sterpin E, Salvat F, Olivera G, et al. (2009) Monte Carlo evaluation of the convolution/superposition algorithm of Hi-Art™ tomotherapy in heterogeneous phantoms and clinical cases. *Med Phys*, **36(5)**: 1566-75.
- Javedan K, Zhang G, Mueller R, et al. (2009) Skin dose study of chest wall treatment with tomotherapy. *Jpn J Radiol*, **27**: 355-62.
- Higgins PD, Han E, Yuan J, et al. (2007) Evaluation of surface and superficial dose for head and neck treatments using conventional or intensity-modulated techniques. *Phys Med Biol*, **52(4)**: 1135.
- Qi ZY, Deng XW, Huang SM, et al. (2009) In vivo verification of superficial dose for head and neck treatments using intensity-modulated techniques. *Med Phys*, **36(1)**: 59-70.
- Wang L, Cmelak AJ, Ding GX (2018) A simple technique to improve calculated skin dose accuracy in a commercial treatment planning system. *J Appl Clin Med Phys*, **19(2)**: 191-7.
- Hauri P, Verlaan S, Graydon S, et al. (2014) Clinical evaluation of an anatomy-based patient specific quality assurance system. *J Appl Clin Med Phys*, **15(2)**: 181-90.
- Abedi Firouzjah R, Nickfarjam A, Bakhshandeh M, et al. (2019) The use of EBT3 film and Delta4 for the dosimetric verification of Eclipse™ treatment planning system in a heterogeneous chest phantom: an IMRT technique. *Int J Radiat Res*, **17(2)**: 355-61.
- Atiq M, Atiq A, Iqbal K, et al. (2017) Interpretation of gamma index for quality assurance of simultaneously integrated boost (SIB) IMRT plans for head and neck carcinoma. *Polish J Med Phys Eng*, **23(4)**: 93-7.
- Grégoire V and Mackie T (2011) State of the art on dose prescription, reporting and recording in Intensity-Modulated Radiation Therapy (ICRU report No. 83). *Cancer Radiother*, **15(6-7)**: 555-9.